Measurement of Plasma Flows Using Mach Probe Array

by

Brian Kardon

Submitted to the Department of Physics
in partial fulfillment of the requirements for the degree of

Bachelor of Science in Physics

at the

MASSACHUSETTS INSTITUTE OF TECHNOLOGY

June 2008

Author .....
Department of Physics
May 20, 2008

Certified by .....
Jan Egedal
Assistant Professor
Thesis Supervisor

Accepted by .....
David E. Pritchard
Senior Thesis Coordinator, Department of Physics

Measurement of Plasma Flows Using Mach Probe Array

by

Brian Kardon

Submitted to the Department of Physics
on May 16, 2008, in partial fulfillment of the
requirements for the degree of
Bachelor of Science in Physics

Abstract

A rectangular array of three-dimensional Mach probes is constructed and installed in the plasma vessel of the Versatile Toroidal Facility (VTF) at MIT in order to measure ion flow velocity on the cross section of the VTF. The probes are tested using well-characterized toroidal plasma 'blobs' in order to determine the array's functionality and applicability to measuring ion flow during reconnection events in the VTF. The Mach probe is used to infer the radial speed of the blobs, and the blob speeds are measured independently by a Langmuir probe array. Using the blob velocity dataset from the Langmuir array as a reference with which to compare the Mach probe data, the theory of unmagnetized Mach probes is be tested. Additionally, the inverse proportionality between blob speed and neutral pressure shown to exist in a previous study of blobs in the VTF is confirmed by Mach probe data. Finally, data from the array show that the blobs are rotating clockwise with Mach numbers of between 0.1 and 0.2, although the mechanism driving this rotation is unknown.

Thesis Supervisor: Jan Egedal
Title: Assistant Professor

Acknowledgments

Special thanks to my parents, Noam Katz, Will Fox, Lissa Riley, Mark Avara, and to Sondy Springmann. Recognition is also due to $C_8H_{10}N_4O_2$.

Contents

List of Figures

List of Tables

Chapter 1

Introduction

The Earth is a remarkable island of cool, neutral matter in the universe. Humanity has only recently begun to understand the state of the matter in the universe outside the lower atmosphere. We have discovered that the vast majority of the matter we observe in the universe is not in the solid, liquid, or gaseous states familiar to terrestrial life, but instead is in a curious fourth state in which a significant fraction of atoms are dissociated from their outer electrons - a plasma. Plasmas are responsible for an incredible menagerie of astrophysical phenomena. Since the plasma is made of a gas of positive and negative charges, plasma responds to and interacts with magnetic and electric fields, which adds an extra six dimensions to the plasma phase space. Ever since scientists learned how to access this regime of matter on the scale of 10 eV or higher in the laboratory, the applications of advances in our understanding of plasma physics have been endless, and the potential applications are even more amazing - from clean waste remediation to interstellar propulsion to fusion energy.

However, plasma presents some uniquely difficult challenges to researchers seeking to measure its properties in the laboratory. For instance, plasmas are hot, and at sufficiently high densities, they can deposit enough heat to vaporize any material put into or around them, including containment vessels or probes. Additionally, since plasmas are locally charged, they interact strongly with electromagnetic waves. This property makes the probing of the interior behavior of plasmas complicated, although it also offers unusual diagnostic opportunities. Also, any electrical measurements of

the plasma tend to perturb the plasma in some way, which can complicate any effort to learn about the unperturbed state of the plasma [9]. In fact, the development and understanding of plasma diagnostics is a very rich field of research; the difficulty of actually observing what is going on inside a plasma is a major roadblock in the development of devices like tokamaks. This thesis concerns the development of an array of probes for use in the Versatile Toroidal Facility (VTF) of the Plasma Science and Fusion Center (PSFC) at MIT. These particular probes are Mach probes, which are designed to measure the three-dimensional ion drift velocity on the cross section of the VTF plasma vessel (see Figure 2-2. The ion drift velocity, sometimes more casually referred to as the plasma velocity or plasma flow velocity, is a measure of the mass-flow of the plasma. The Mach probe specifically measures the 'Mach number' M of the plasma, which is the plasma flow velocity divided by the ion sound speed c_s

$$M \equiv \frac{v_{flow}}{c_s} \tag{1.1}$$

where $c_s = \sqrt{\frac{T_e+T_i}{m_i}}$ and m_i is the mass of the ions. The plasma Mach number is often an important vector quantity to measure for plasma research. Electric, magnetic, and density measurements can describe and explain a good deal of the activity in a plasma. However, they are sometimes insufficient, especially in regions and regimes of plasmas where neither resistive MHD nor collisionless theory is entirely valid, such as near the X-point of a reconnection event, or in other situations that involve complex flows. In cases such as these, it is very useful to measure plasma flows directly, and the most direct tool for measuring plasma flow is the Mach probe.

A Mach probe consists of two mutually isolated conductors inserted adjacently in the plasma; essentially a Langmuir probe where the two halves of the probe do not communicate. This allows a measurement of an 'upstream' and 'downstream' probe current in the plasma flow. If the plasma is non-stationary, the upstream and downstream halves of the probe will draw different currents. It can be shown that the Mach number of the plasma is a function of the two probe currents. If three of these Mach probes are constructed together, they can be used to measure the

three-dimensional plasma flow at a point in the plasma. A convenient probe setup able to measure the three dimensional Mach number in a plasma could illuminate the complex process of magnetic reconnection.

A Mach probe array has been built and installed at the VTF for the purpose of observing flows during induced reconnection events in a toroidal plasma vessel. The probe is designed to measure the three-dimensional Mach number at various points on a cross section of the vessel. Mach probe theory is complicated by the fact that varying ion and electron temperatures, magnetic field strengths, and plasma Mach numbers produce very different probe behavior; no unifying model covers all ranges of those plasma parameters. Using plasma 'blobs' generated within the VTF plasma vessel, I will study and characterize the operation of the Mach probes in reference to the various theories and simulated results available in Mach probe literature by comparing the Mach numbers predicted by theory and simulation to independent measurements of blob velocity by Langmuir probe arrays in the VTF.

Chapter 2

Experimental Setup

2.1 The Versatile Toroidal Facility

The Versatile Toroidal Facility (VTF) plasma vessel is a stainless-steel toroidal chamber of rectangular cross section, diagrammed in Figure 2-2. The radius to the inner wall is $0.62m$. Poloidal cross sections (cross sections made by a vertical plane containing the axis of the toroidal plasma vessel) of the chamber are rectangular, with a radial width $0.64m$ and a height of $1.08m$. In the VTF machine, an low-density argon plasma is created by a 2.45 GHz, 15 kW microwave source. Eighteen copper coils produce a toroidal magnetic field in the vessel, and various other coils are available to produce different magnetic field geometries. In Figure 2-1, a photograph of the VTF illustrates the arrangement of the exterior of the vacuum vessel and equipment.

2.1.1 Blob configuration

While the VTF is set up primarily to induce magnetic reconnection for the purpose of studying reconnection processes, it can also operate in a different mode to produce plasma filaments, or blobs. These blobs, which have been extensively characterized by a previous study at the VTF [4], are tori of plasma which propagate radially due to the force balance between the centrifugal force on the electrons and the collisional drag between the blob plasma and the surrounding neutral gas. Their structure and

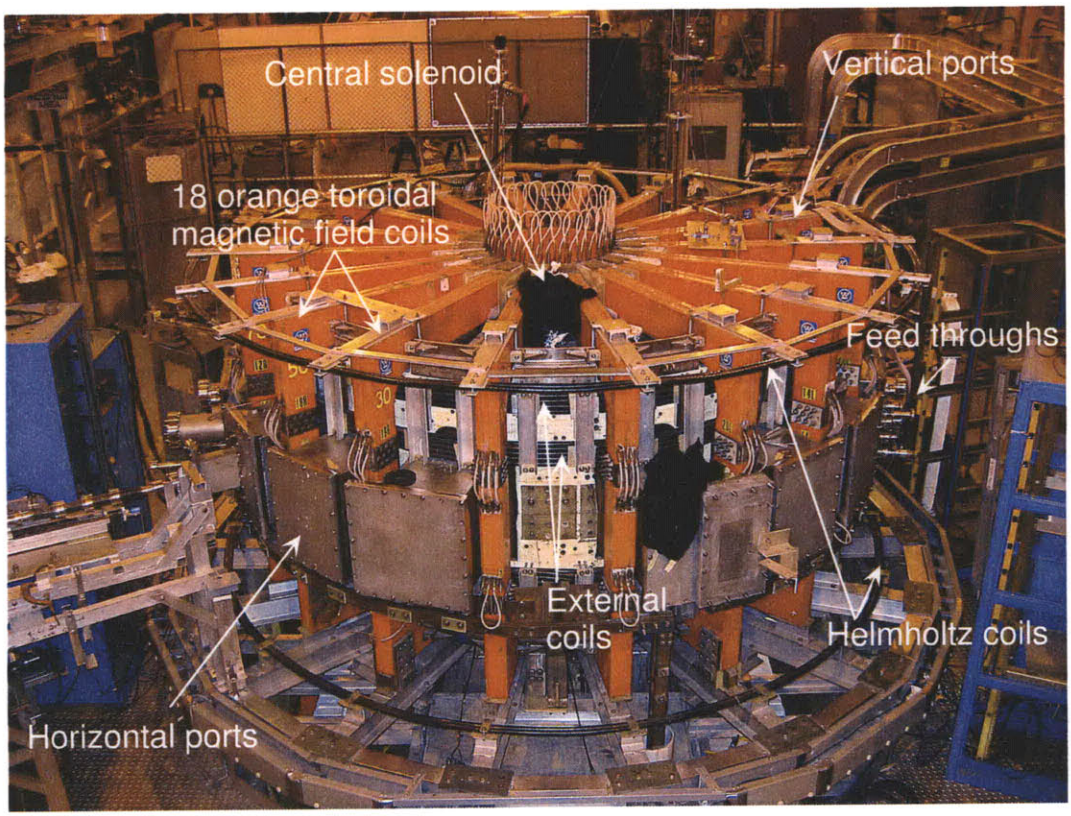

Figure 2-1: A photograph of the exterior of the VTF plasma machine, illustrating the layout of equipment and the vacuum vessel.

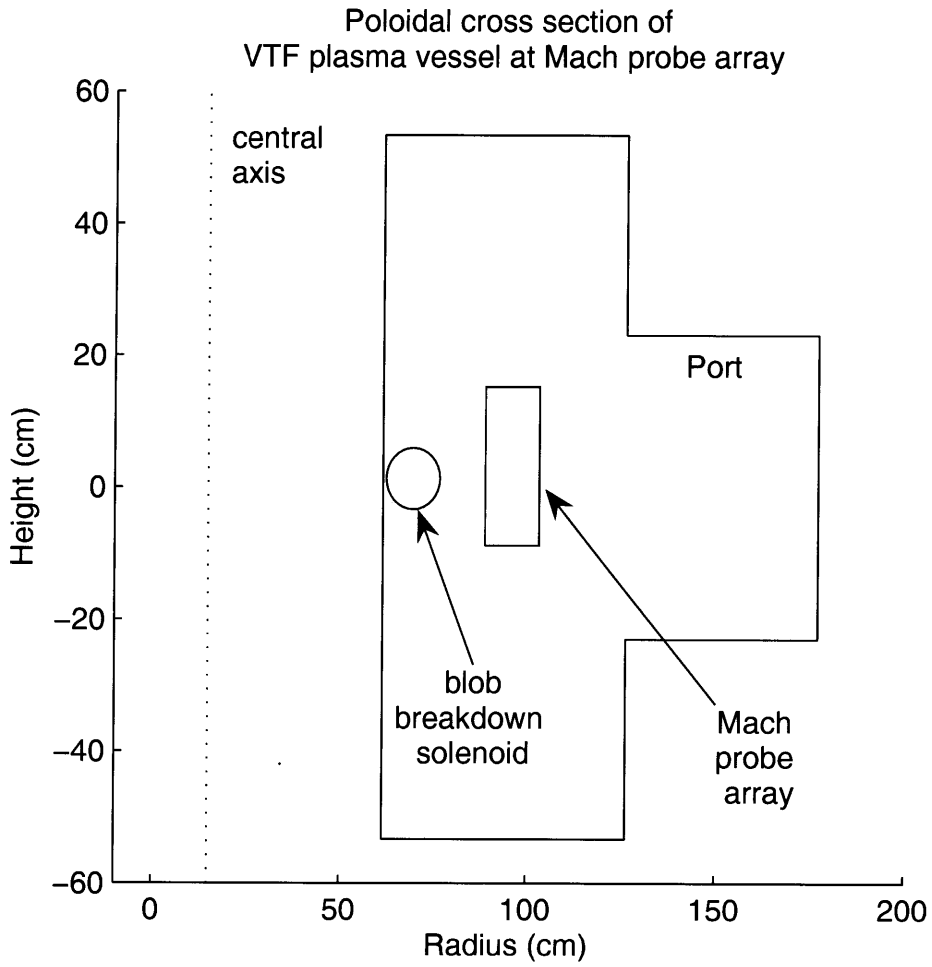

Figure 2-2: A diagram of a poloidal cross section of the Versatile Toroidal Facility at the toroidal angle at which the Mach probe array is installed, showing the plasma vessel walls and other equipment.

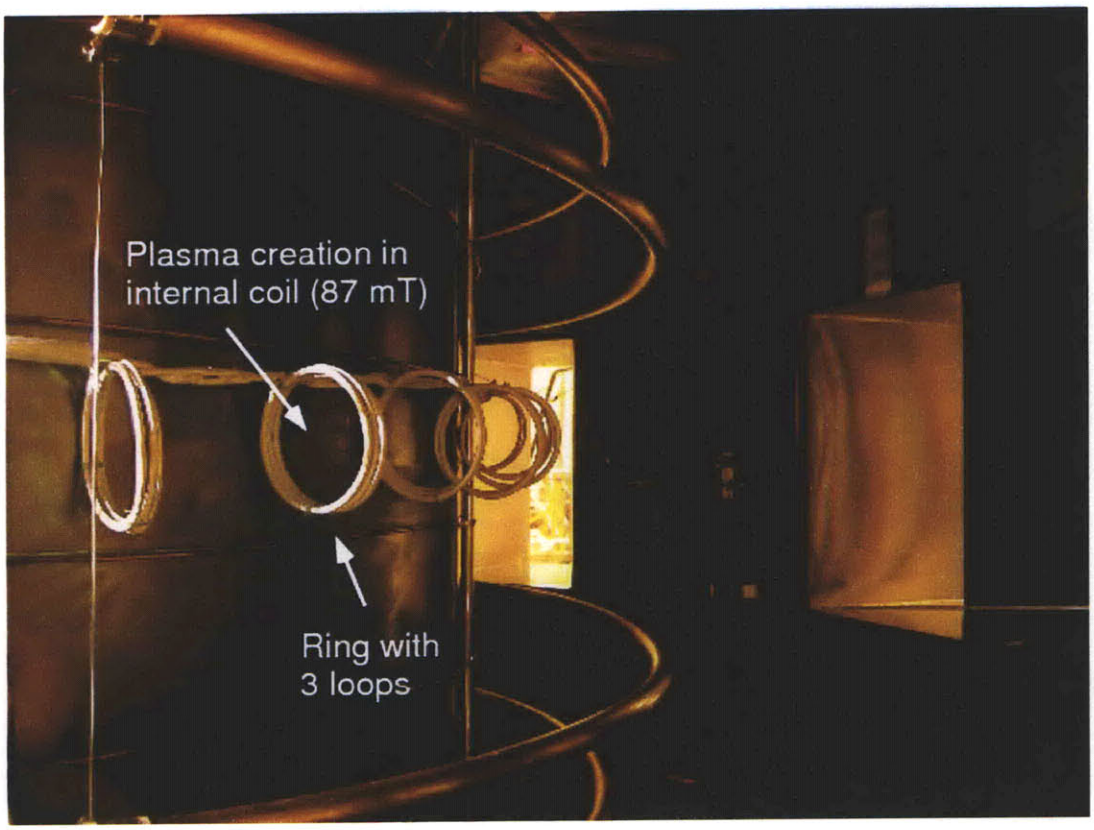

Figure 2-3: A photograph of a section of the magnetic coil around the central trunk of the plasma vessel in which the plasma blobs are formed. This coil locally increases the magnetic field in order to bring the electron cyclotron breakdown frequency up to the VTF microwave frequency of 2.45 GHz.

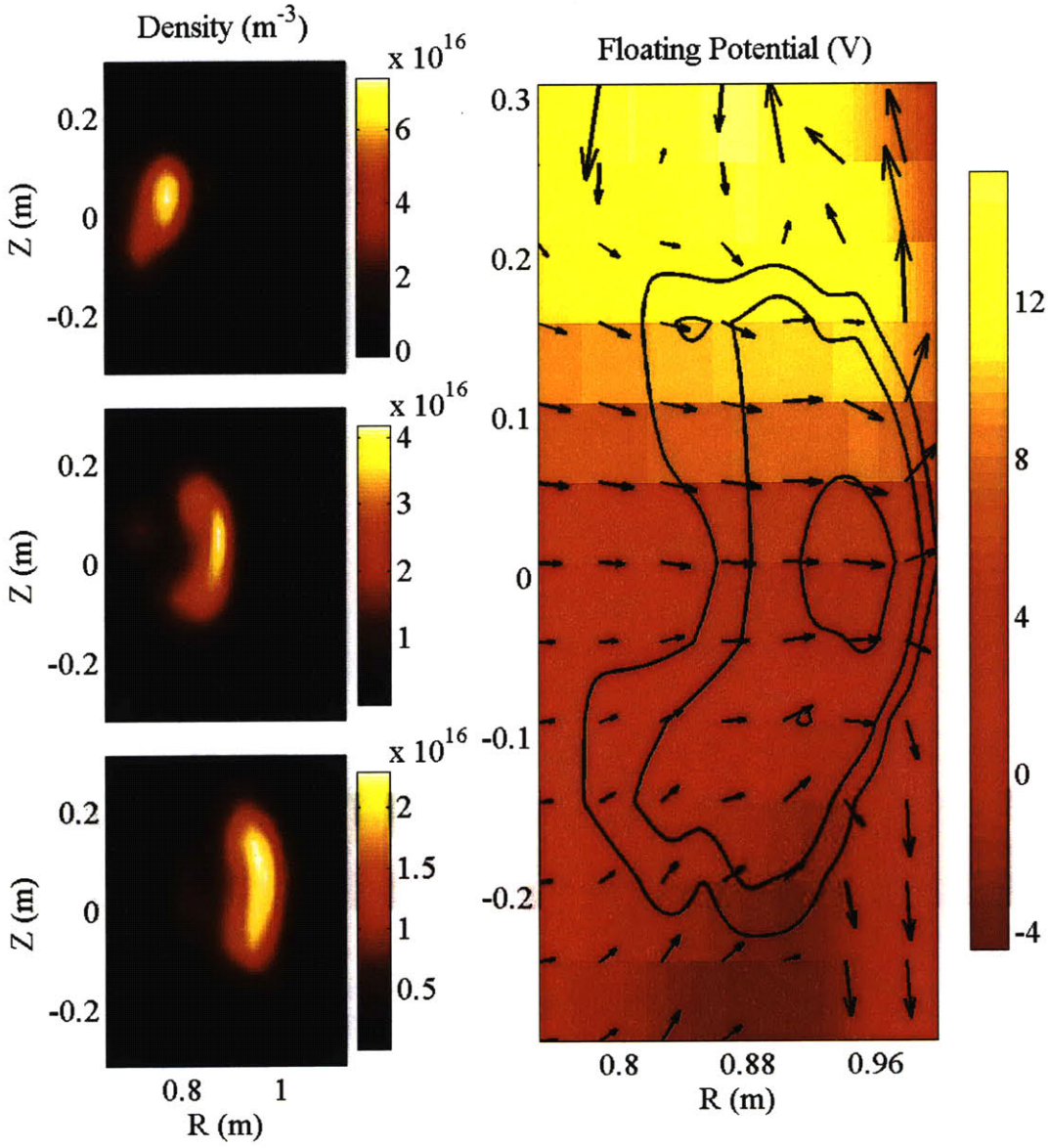

Figure 2-4: This figure is taken from [4]. On the right is a detailed poloidal cross section (a cross section made by a vertical plane containing the central axis of the toroidal plasma vesssel) of a typical blob showing floating potential in the color dimension, plasma density in the contour plot, and the ExB vector demonstrating the source of the radial drift of the blob. On the right is a sequence of the blob at three different times showing the propagation.

Table 2.1: Properties of blob plasmas

Property	Value
Plasma Density n	$2 \cdot 10^{-5}$ Torr - $4 \cdot 10^{-3}$ Torr
Ion temperature T_i	0.5 eV - 1.0 eV
Electron temperature T_e	1.0 eV - 3.0 eV
Breakdown toroidal field $B_{breakdown}$	87 mT
Peak main toroidal field B_0	40 mT

propagation are illustrated in Figure 2-4, taken from the aforementioned paper, and the properties of the blob plasma are summarized in Table 2.1.

In this thesis, the VTF was used to create plasma 'blobs' (sometimes referred to as plasma filaments in literature). A plasma blob is a coherent region of elevated plasma density in a background of neutral gas or a less dense plasma. Blobs often occur in astrophysical plasmas, and in edge regions of magnetically confined fusion devices. During the production of blobs in the VTF, toroidal field magnets produce a mid-chamber magnetic field of $B_0 = 40$ mT. A small solenoid wrapped around the inner wall of the chamber at mid-height (see Figure 2-3) augments the main toroidal field to a value of $B_{breakdown} = 87$ mT. This allows the 2.45 GHz microwave power to resonate with the electron cyclotron motion and break down the gas into plasma inside (and only inside) the volume of the small solenoid. This creates a toroidal region of plasma, a 'blob', which propagates radially outward through a background of neutral argon gas. In the process, it passes through several Langmuir and magnetic probes, as well as the Mach probe array. These blobs are very useful for the testing, calibration, and characterization of the operation of the Mach probe array because they are quite well defined and reproducible, and, compared to the plasma dynamics in the VTF during reconnection shots, their structure is simple.

2.2 The Mach Probe Array

The Mach probe array constructed for this thesis is a 3 x 5 rectangular array, as seen in Figure 2-5. Each array node is a fiberglass cube 0.6 cm on a side. The cubes

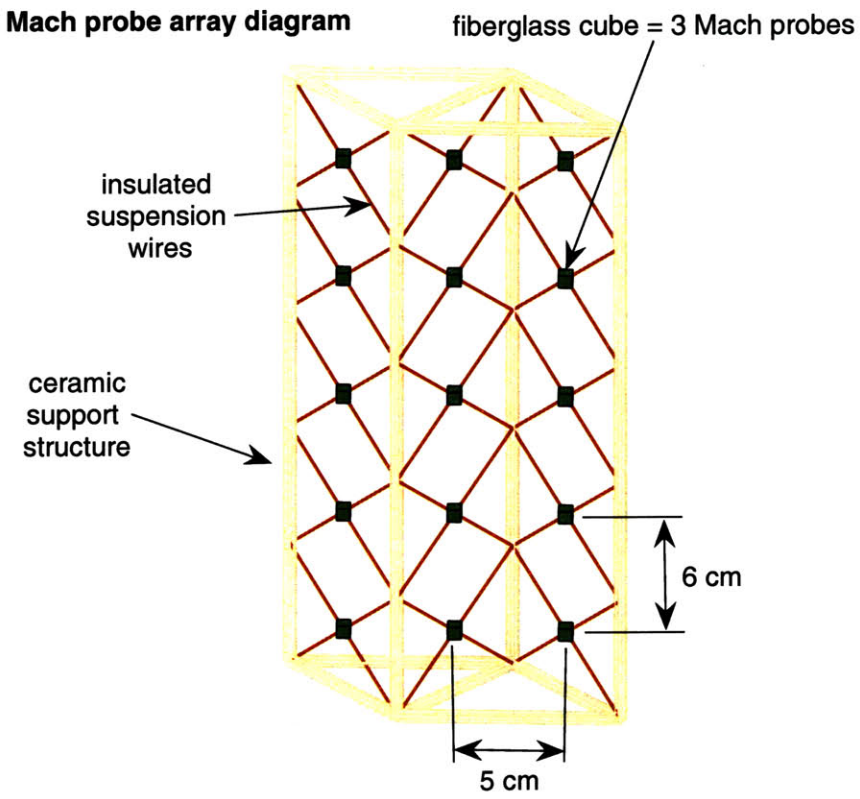

Figure 2-5: A diagram of the constructed Mach probe array.

were constructed from printed circuit boards (PCBs) machined into square faces and assembled with a vacuum sealant (Torr Seal). Each of the six sides of the cubes features a circular metal PCB pad with diameter 0.2 cm. The cubes are suspended from a frame of ceramic rods by insulated wires.

The six signals from the six faces of each of the cubes are carried by 0.004" diameter wires along the support structure, through a vacuum feedthrough, then to a digitizer where the probe currents (measured via the voltage across a resistor) are recorded and stored. Each pad, together with the corresponding pad on the opposite side of the cube, forms a Mach probe; I will therefore refer to the pads as the 'probe faces'. The result is that each cube functions as three Mach probes together, each facing a different orthogonal direction. Thus the Mach probe array provides a three dimensional array of points in the plasma at which the three-dimensional Mach vector may be measured.

Chapter 3

Theory

3.1 Langmuir probe theory

The Mach probe is essentially an elaboration on the Langmuir probe. The Langmuir probe consists simply of a conductor suspended in the plasma, presumably attached to an insulated signal wire to transmit the probe current for measurement. The Langmuir probe is a very useful tool for measuring plasma; it can be used to determine plasma density, as well as other useful parameters such as electron temperature T_e. An understanding of Langmuir probe operation is a good basis for understanding Mach probe operation, so I will now seek to characterize the current drawn by Langmuir probes for different plasma and probe conditions. In particular, I wish to calculate some of the important points and features in the I-V curve of the probe, an example of which is shown in Figure 3-1. This curve, which gives the current emitted by the probe for any bias voltage applied to the probe, is also known as the 'probe characteristic'.

Consider a plasma with ion and electron densities n_i and n_e and some electron and ion temperatures T_e and T_i. We will only consider collisionless plasmas, which are plasmas in which the mean free path of particles is large in comparison to the probe dimensions, so that particles arrive at the probe in free flight, rather than diffusively [9]. Since the plasmas dealt with in this thesis are quite low density, the collisionless condition is satisfied.

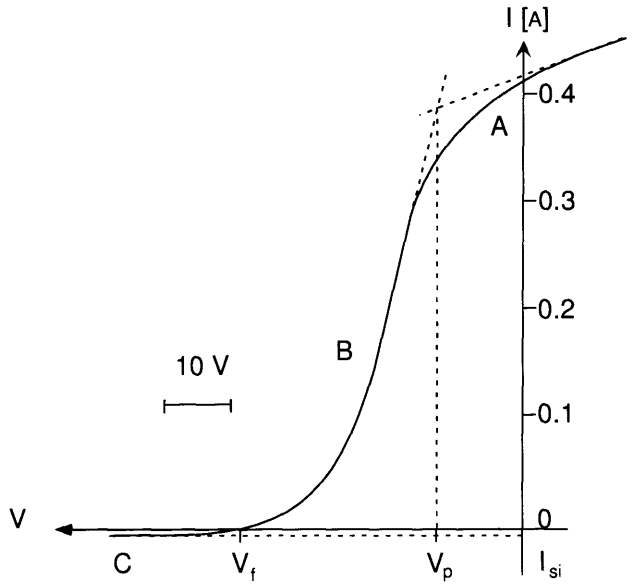

Figure 3-1: The I-V curve for a Langmuir probe; this shows the current emitted by the probe for a particular bias voltage. The voltage scale is defined up to a constant offset, since the plasma potential is not known a priori.

Suppose we place a spherical conductor, i.e. a Langmuir probe, of surface area A in this plasma, and initially wish to find the current to the probe when it does not perturb the plasma at all. That is, we maintain the probe at the same electric potential as the potential of the plasma before we inserted the probe; this potential is known as the 'plasma potential', V_p. A simple statistical calculation can show that the flux of either electrons or ions across an arbitrary surface in the plasma, for instance the surface of this probe, is given by

$$\Gamma_i = \frac{1}{4} n_i \bar{v}_i, \quad \Gamma_e = \frac{1}{4} n_e \bar{v}_e \tag{3.1}$$

where $\bar{v}$ is the average, or thermal velocity, the velocity of particle with kinetic energy equal to the average thermal energy T (note that here and in the rest of this thesis I will write temperatures in units of energy), so

$$\bar{v}_i = \sqrt{\frac{2T_i}{m_i}}, \quad \bar{v}_e = \sqrt{\frac{2T_e}{m_e}} \tag{3.2}$$

Thus the total current emitted by the probe is given simply by

$$\begin{aligned} J_{probe} &= -eA\left(\Gamma_i - \Gamma_e\right) \\ &= \frac{1}{4}eA\left(n_i\bar{v}_i - n_e\bar{v}_e\bar{v}_i\right) \\ &= \frac{\sqrt{2}}{4}eA\left(n_i\sqrt{\frac{T_i}{m_i}} - n_e\sqrt{\frac{T_e}{m_e}}\right) \\ &\approx \frac{\sqrt{2}}{4}eAn_e\sqrt{\frac{T_e}{m_e}}, \quad \frac{T_e}{m_e} \gg \frac{T_i}{m_i} \end{aligned} \tag{3.3}$$

For any reasonable T_e and T_i, the enormous mass difference between electrons and ions makes the approximation in 3.3 accurate. This leads to a somewhat unintuitive result; an isolated conductor in a plasma at the plasma potential will draw a negative current (or according to the convention, emit a positive current)!

Now suppose that instead of holding the probe at V_p, we isolate the probe from everything except the plasma. Since the probe is drawing a negative current, the probe will quickly gain a negative charge and the probe voltage will drop. This will continue until the probe voltage is sufficiently negative to repel enough electrons and attract enough ions to equalize the ion and electron fluxes ($\Gamma_i = \Gamma_e$) and bring the current to zero. The voltage at which that occurs is known as the 'floating' potential V_f, since any conductor 'floating', or isolated, in the plasma will attain this voltage. The floating voltage is marked in Figure 3-1 where the I-V curve crosses the I = 0 line.

If we again apply a voltage, or bias, to the probe, we can determine more of the I-V curve. If we decrease the bias below V_f, we will repel more electrons and attract more ions so qualitatively it is clear the the emitted current will become negative. As we set V_{probe} more and more negative, we should expect that the emitted current will eventually stop decreasing and plateau; for a sufficiently negative V_{probe}, essentially all of the electrons are repelled (only electrons with energies in the thin tail of the Maxwell-Boltzmann distribution escape the probe), and all of the incident ions are collected, and the current cannot decrease any more. This region is known as the ion saturation region, and the current emitted by the probe in this region is known

as the ion saturation current. Similarly, we would expect that if we bias the probe to a sufficiently positive potential the current will eventually plateau when nearly all incident electrons are collected and nearly all ions are repelled. This current is known as the electron saturation current.

It is interesting to note that the current does not entirely stop changing in either saturation region. The reason for this is found in the idea of an effective collecting surface of the probe. The effective collecting area of the probe is the area of a small region around the probe in which particles that enter are trapped by the probe's potential well. For instance, in ion saturation, ions whose trajectories take them near the probe are drawn in by the electric field of the probe. The region where this occurs is known as the probe sheath.

An important property of plasmas is that they tend to attenuate electric fields. Since plasmas are made of free charges, any electric fields in the plasma cause the ions and electrons to redistribute themselves to reduce the electric field. We can see this by considering Poisson's equation in a plasma:

$$\nabla^2 V = -\frac{\rho}{\epsilon_0} \tag{3.4}$$

$$= -\frac{e}{\epsilon_0}(n_i - n_e) \tag{3.5}$$

If we again consider a spherical probe, the density of electrons as a function of radial distance r from the probe is given by Boltzmann statistics [1]:

$$n_e(r) = n_e(r = \infty)e^{\frac{eV(r)}{T_e}} \tag{3.6}$$

We will assume that the heavy ions do not significantly redistribute themselves, so their density is constant; $n_i(r) = n_i$ [9]. Substituting this and Equation 3.6 into Equation 3.4, we obtain

$$\nabla^2 V = -\frac{e}{\epsilon_0} n \left(1 - e^{\frac{eV(r)}{T_e}}\right) \tag{3.7}$$

where n is the plasma density (both ion and electron density) far from the perturbing probe where the plasma is neutral. If we assume $eV \ll T_e$, then we can expand the

exponential to first order to obtain

$$\nabla^2 V = \frac{nVe^2}{\epsilon_0 T_e} \tag{3.8}$$

This equation admits solutions of the form

$$V(r) = V(0)e^{-\frac{r}{\lambda_D}} \tag{3.9}$$

where $\lambda_D = \sqrt{\frac{\epsilon_0 T_e}{ne^2}}$ is known as the Debye length; it is the characteristic length for the attenuation of an electric potential and electric field in a plasma. The sheath, which is the effective collecting surface for a Langmuir probe, is generally considered to extend a few Debye lengths out from the actual probe surface. For the plasmas considered in this thesis, the Debye length is generally much smaller than the dimensions of the probes.

3.2 Mach probe theory

The characteristics of plasmas vary wildly with ion and electron temperature, density, magnetic field strength, composition, and measurement length scale. Even within achievable laboratory plasmas (a paltry subset of the plasmas available to astrophysics), it is difficult to make general statements about the behavior of a plasma or a plasma probe without carefully describing the plasma of interest and the probes used to measure it. The properties of the VTF blob plasma were summarized in Table 2.1. I will now proceed to describe how the plasma interacts with the probe to produce a meaningful signal current.

3.2.1 Ion saturation

The Mach probes are operated in the ion saturation regime (see Section 3.1). That is, the Mach probes are biased at a potential which is negative enough relative to the plasma potential that nearly all the electrons are repelled from the probe, and

all the ions that enter the probe sheath are captured. This will allow the probes to measure the ion velocities without considering the effect of the electron flux to the probes. An advantage of the ion saturation regime is that the probe signal is nearly independent of bias voltage; changes in voltage cannot cause more electrons to be repelled or more ions to be captured. The probes were biased at $V_{bias} = -90$ V with respect to ground (the vessel wall). The electron density at the probe surface, a rough measure of the density of electrons collected by the probe (which we wish to minimize in ion saturation) is given by Equation 3.6 evaluated at $r = 0$. For an electron temperature of $T_e \approx 2$ eV and a voltage at the surface of $V(r = 0) = -90$ V, we obtain an extremely small ratio of $n_e(r = 0)/n_e(r = \infty) = 3 \cdot 10^{-20}$, meaning the probes collect virtually no electrons.

3.2.2 Unmagnetized regime

The ions in the VTF plasma are unmagnetized on the scale of the probes. That is, the radius of the probe faces r_{probe} is significantly smaller than the ion larmor radius r_i^ω; essentially the motion of the ions is not dominated by the magnetic cyclotron motion, and the ions can be treated thermally. The Mach probe faces have radii $r_{probe} = 0.2$ cm. The effective collecting surface of the probe face is actually the sheath surface (the edge of the plasma region through which the electric field from the probe penetrates), but as the Debye length is on the order of $10\mu m$, r_{probe} is an satisfactory approximation. Since the ion temperature is in the range $T_i = 0.5 - 1$ eV, the ion cyclotron radius r_i^ω, given a field strength of $B \approx 40$ mT, is $r_i^\omega = \frac{m_i \bar{v}_i}{q_i B} \approx 2.4$ cm, and indeed $r_i^\omega > r_{probe}$.

The theory of magnetized plasma flow measurement is somewhat more developed, perhaps partly because it is theoretically simpler. In a plasma which is magnetized, the close confinement of ion movement along magnetic field lines makes it natural to divide the plasma into two regions; the first is a cylindrical region extruded along the magnetic field lines from each half of the Mach probe, and the second is all of the plasma outside that region. The cylindrical region is known as the 'presheath', and in ion saturation the current from the presheath is simply found from a one dimensional

kinetic treatment. All the plasma outside the 'presheath' can be described as a source of particles diffusing into the presheath [9], essentially reducing the plasma to a one-dimensional system. Unmagnetized Mach probe theory is less firmly characterized, although there have been several recent experimental and theoretical studies which have arrived in agreement.

3.3 Models for Mach probe signals

Several models of Mach probe signals from plasma flows for unmagnetized plasmas have been developed in the past. In general, they all seek to relate the plasma Mach number M to the "upstream" and "downstream" currents j_a and j_b drawn by each Mach probe pair. In a 2002 paper [8], Hutchinson conducted an extensive particle in cell (PIC) simulation of an unmagnetized Mach probe to determine this relationship. In the process he reviewed several of the more famous results and compared them to the simulation. I will now discuss some of these theories and results and how they can be tested by the Mach probe data and the Langmuir probe data. Unfortunately, limited knowledge of T_i and T_e in the blobs curtails our ability to experimentally distinguish between the models. Additionally, most of the literature focuses on the behavior of a spherical mach probe (that is, one constructed from two mutually insulated halves of a sphere), whereas the Mach probe studied in this thesis is a separated parallel plate probe - it is unclear what effect the differing geometry might have. However, the validity of the overall model can be verified, and some instructive observations can be made. All of the theories express the ratio of the Mach probe upstream and downstream currents as follows:

$$\frac{j_a}{j_b} = e^{KM} \tag{3.10}$$

Or, rearranging,

$$M = \frac{1}{K} \ln\left(\frac{j_a}{j_b}\right) \tag{3.11}$$

Here K is a 'calibration constant', which generally is likely to be dependent on T_e and T_i. It is the determination of K for different plasma temperatures which is the focus of the theory and simulation work on unmagnetized Mach probes. A longstanding model by Hudis and Lidsky [6] developed from a one-dimensional ion kinetic analysis arrives at

$$K = \frac{\sqrt{32\ T_i(T_i + T_e)}}{T_e} \tag{3.12}$$

For the estimated $T_i \approx 0.5eV$ and $T_e \approx 2eV$, this gives a calibration constant of $K \approx 3.16$.

Hutchinson's simulation arrived at a value of $K = 1.34$ for values $\frac{T_i}{T_e} \leq 3$; this value is shown to be accurate within 10% for that range. Studying the published results for lower temperature ratios, Hutchinson's data appears to suggest that for lower temperature ratios, the appropriate calibration constant may be slightly higher - a fit to the published data for the temperature ratio of $\frac{T_i}{T_e} \approx 0.2$ gives a value of $K = 1.7$. Ando [2] conducted an experiment using plasma arcjets subsequent to Hutchinson's simulation and found his experimental results to be consistent with Hutchinson's simulation.

In this thesis, I generally use a slightly different model for analytic simplicity. However, it can be shown that the two models are for specific approximations algebraically equivalent. The model used in most of the calculations in this thesis is as follows:

$$M = \frac{j_a - j_b}{j_a + j_b} \tag{3.13}$$

We can show that this is equivalent to Equation 3.11:

$$\begin{aligned} M &= \frac{1}{K} \ln\left(\frac{j_a}{j_b}\right) \\ &= \frac{1}{K} \ln\left(1 + \frac{j_a - j_b}{j_b}\right) \\ &\approx \frac{1}{K} \frac{j_a - j_b}{j_b} \quad \left(\frac{j_a - j_b}{j_b} \ll 1\right) \\ &= \frac{j_a - j_b}{K j_b} \end{aligned} \tag{3.14}$$

$$\approx \frac{j_a - j_b}{j_a + j_b} \quad \left(K = \frac{j_a + j_b}{j_b} \approx 2 \right) \tag{3.15}$$

In order for this model to be consistent with Equation 3.10, we must fix the calibration constant at $K \approx 2$. In fact, I will later show (in Figure 4-7) that for the cubical probe geometry, and for the T_i and T_e of the blobs, this model is accurate.

Chapter 4

Data Analysis and Results

During each shot, the Mach probe signal is digitized at a rate of 2 MHz. With six signals from each of the fifteen array nodes, a total of $1.8 \cdot 10^6$ samples are recorded, so significant automation was required in interpreting and analyzing the signals. The processing steps are discussed in more detail in Chapter 4.1. The Mach probe array data recorded during a typical blob shot is displayed in Figure 4-1. The plots are arranged in the relative geometry of the probes that generated them; viewed this way, the plasma blob can be observed to pass the inner probe column first, then propagate outward. Even from the raw signals, the radially inward and radially outward faces can be observed to have signals of significantly different magnitude - it is this difference that is interpreted as a radial plasma flow.

Since the processing steps required to take the raw Mach probe signals and transform them to meaningful plasma flow data is non-trivial, I will first explain those steps in detail before moving on to discuss experimental results.

4.1 Data Processing and Error Analysis

4.1.1 Signal noise reduction

There are several sources of noise in the signal pathway from the plasma to the digitizer. First, background electrical fluctuations are a constant source of dark current

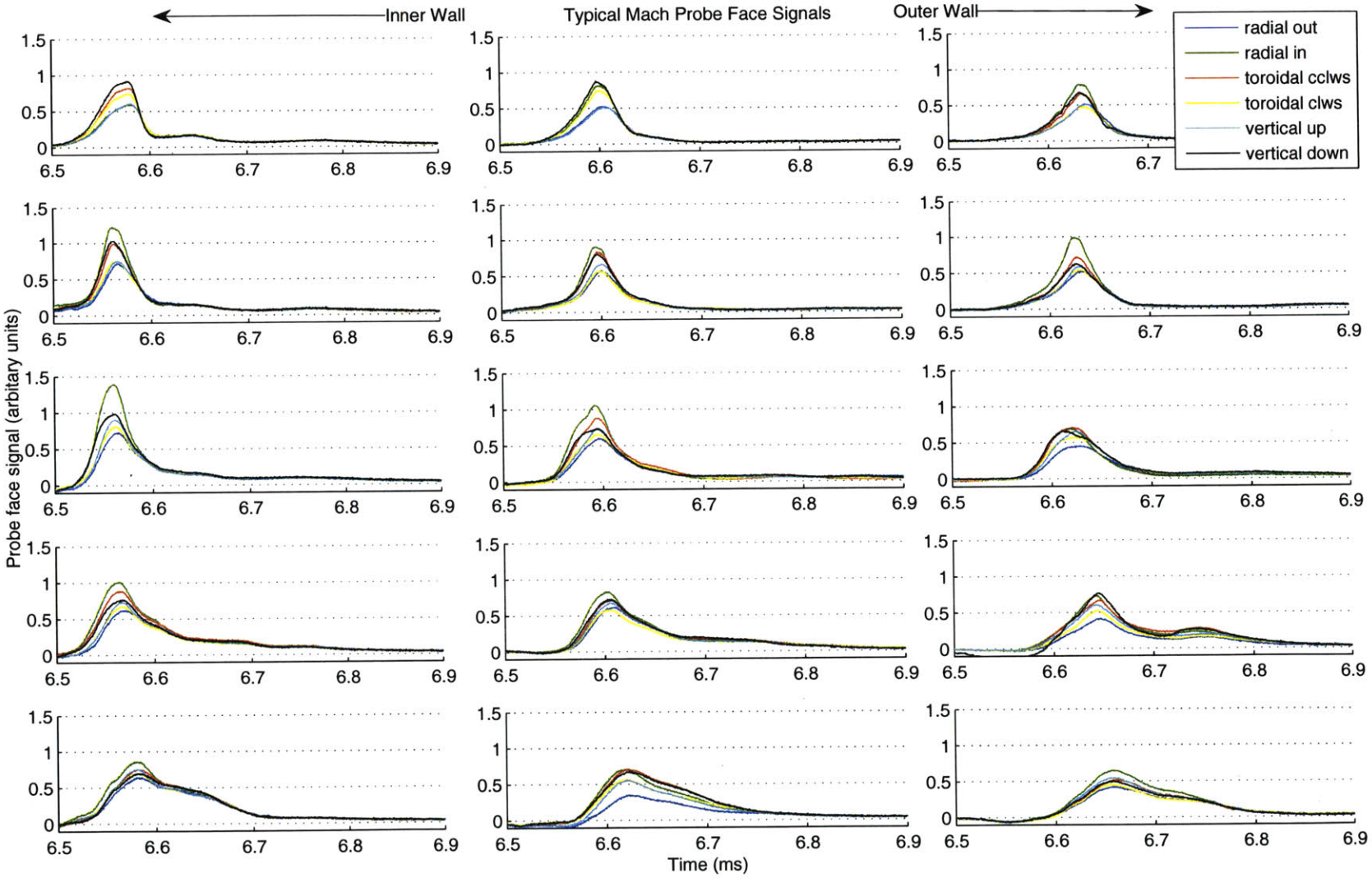

Figure 4-1: Typical signals from a blob passing across the Mach probe array.

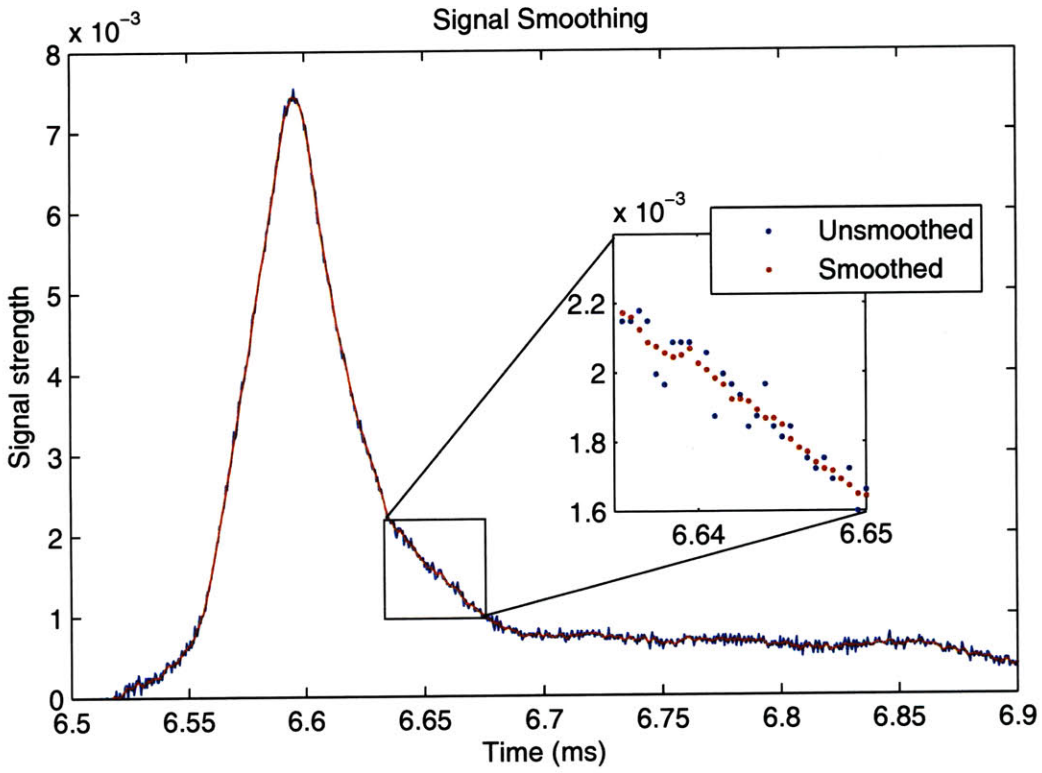

Figure 4-2: A demonstration of smoothing the raw data with a smoothing kernel of width 5.

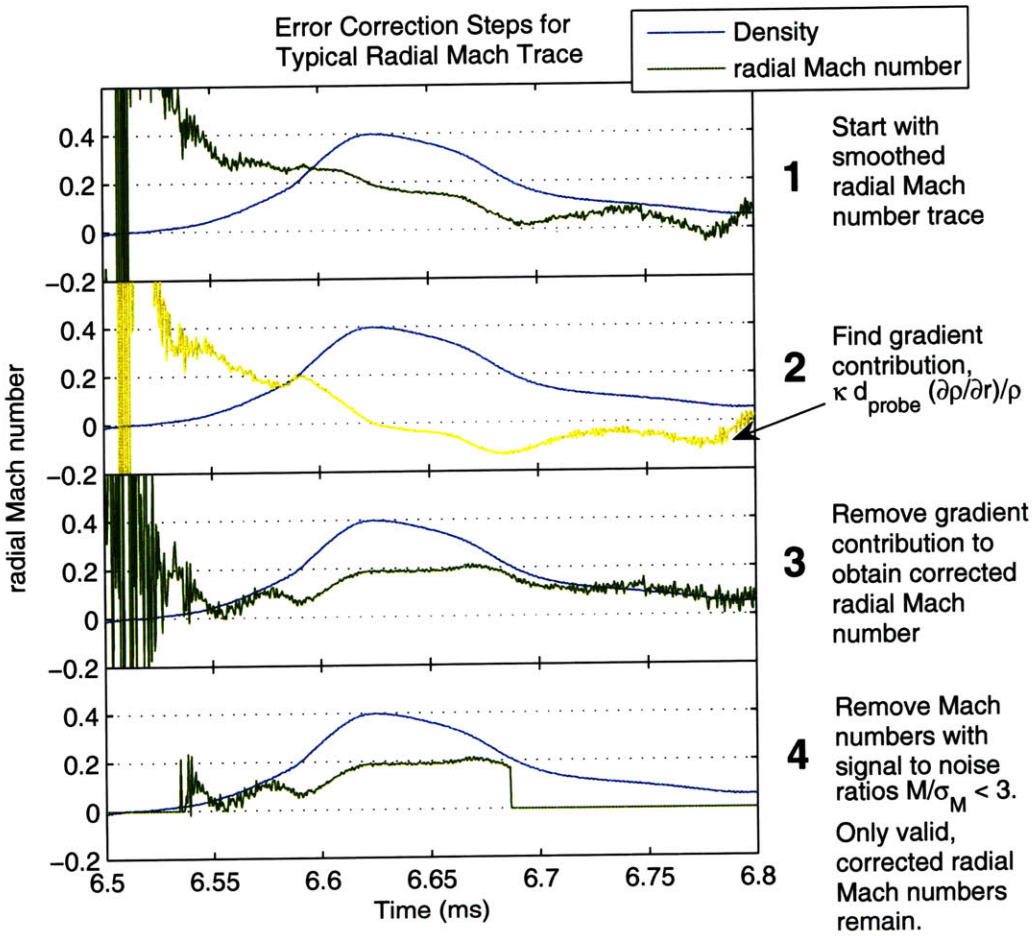

Figure 4-3: An illustration of the error processing steps for Mach numbers. The density is plotted for reference in arbitrary units.

noise, present even in the absence of plasma. This background noise is very troublesome in the calculation of the Mach number. The first step to take is to smooth the raw data. A smoothing kernel with a width of five time samples was used. This is illustrated in Figure 4-2.

It is also possible to accurately quantify the Mach number 'signal to error' ratio $\frac{M}{\sigma_M}$ in terms of the spread in the probe signals due to the background noise σ_n.

$$\frac{M}{\sigma_M} = \left(\frac{j_a^2 - j_b^2}{2\sqrt{j_a^2 + j_b^2}} \right) \frac{1}{\sigma_n} \tag{4.1}$$

It is necessary to impose a restriction on the signal to noise ratio, in order to exclude spurious Mach numbers when the density becomes small. A signal to noise ratio of $\frac{M}{\sigma_M} > 3$ appears to be an effective restriction to exclude noise but preserve valid flow readings. This is a particularly crucial piece of analysis; if the Mach probes are used to measure more complicated plasmas without preestablishing this restriction, it would be easy to misinterpret Mach number noise as physical flows. Figure 4-3 shows the process of noise removal applied to the Mach probe signals. There are several other sources of noise, for instance inductive crosstalk between the probe signal wires and other systems involved in creating the plasma. These sources generally manifest as isolated bursts of noise that are easy to identify and remove, although they pose a more serious problem when they interfere with automated processing procedures. Since these types of noise sources generally affect all the probe signals equally and simultaneously, it would be possible to run an extra signal wire to the probe array (insulated from the plasma) and use the signal from that wire to automatically eliminate inductive noise.

4.1.2 Plasma gradient correction

A necessary consideration in the process of analyzing the signal from Mach probes is the effect of the non-zero probe face separation distance $d_{probe} > 0$. When the plasma density ρ varies significantly over the length scale of the collector separation

distance, the Mach probe will produce signals indicating a flow even if the plasma is stationary. That is, when the magnitude of the variation in plasma density over the probe separation distance is on the order of magnitude of the density:

$$\frac{\Delta\rho}{\rho} = \frac{\vec{\nabla}\rho \cdot \vec{d}_{probe}}{\rho} \approx 1 \tag{4.2}$$

For instance, in the case of the plasma blobs, the density gradient is highest on the leading edge of the blob in the radial direction, with a magnitude of $\nabla\rho\cdot\hat{r} \approx 8\cdot10^{17}m^{-4}$. With a probe separation distance of $d_{probe} = 0.6cm$, $\frac{\Delta\rho}{\rho} \approx 0.12$. Therefore, the plasma gradient will induce a significant error in the plasma flow. If we possess a knowledge of the density profile of the plasma, it is possible to analytically correct for this error due to plasma density gradient. By summing the signals from the six faces of each array node, we can get a good approximation of the density of the plasma (essentially using each group of three Mach probes as a single crude Langmuir probe).

Due to the simple propagation dynamics of the blobs, it is possible to infer the radial density profile of the plasma; essentially if we assume that the blob density profile changes much more slowly in the frame of the blob than it does in the laboratory rest frame. A qualitative examination of the Mach and Langmuir array data confirms that this is a reasonable assumption. Therefore, we can think of the blob as an essentially static profile moving radially past the Mach probe array, which means can treat the profile of density with time as a profile of density with radial distance with a scale factor between the time coordinates and space coordinates which is the radial speed of the blob v_{blob}. At that point, it is a simple matter to take the radial derivative in the gradient. That is,

$$\begin{aligned}
\frac{1}{\rho}\nabla\rho \cdot d_{probe}\hat{r} &= \frac{1}{\rho}\frac{\partial\rho}{\partial r}d_{probe} \\
&= \frac{1}{\rho}\frac{\partial\rho}{\partial t}\frac{\partial r}{\partial t}d_{probe} \\
&= \frac{1}{\rho}\frac{\partial\rho}{\partial t}v_{blob}\ d_{probe}
\end{aligned} \tag{4.3}$$

The assumption was then made that the actual radial Mach number should be

approximately constant through the dense center of the blob. Using that assumption, we could determine the appropriate contribution to add to the Mach number trace to correct for the density gradient effects.

$$M(t) = M_{observed}(t) - \kappa \frac{1}{\rho} \frac{\partial \rho}{\partial r} d_{probe} \tag{4.4}$$

By fitting $M(t)$ from Equation 4.4 to a constant in the high-density regions, it was determined that the value $\kappa = 0.7$ consistently produce Mach flow profiles which are approximately constant in time for the high-density regions of the blobs. This process is demonstrated in Figure 4-3.

Ideally a correction like this one would be applied to the vertical Mach numbers as well, since the vertical gradient is nonzero as well, but as the blobs propagate radially, and not vertically, the same detailed knowledge of the vertical density profile was not available. In the future, if sufficiently high-resolution two dimensional density profiles are generated by Langmuir arrays in the VTF machine, it will be possible to use that data to accurately correct for gradient effects in all directions. It should be noted that gradients in plasma parameters other than density (such as electron or ion temperature) could potentially generate similar errors. In fact, the electron temperature is known to decrease somewhat as the blob propagates through the chamber [4], but the effect this could have on the measured Mach numbers is expected to be small. Some unexpectedly high vertical Mach numbers observed within the blobs could be a result of vertical gradients in blob density, but that analysis is not available.

4.2 Results

4.2.1 Mach number data

Figure 4-4 is a plot of the toroidal, radial, and vertical Mach numbers for a representative plasma shot. The apparent toroidal Mach flow is discussed in Section 4.2.4. The abrupt gaps in the Mach number traces are a result of filtering the Mach number

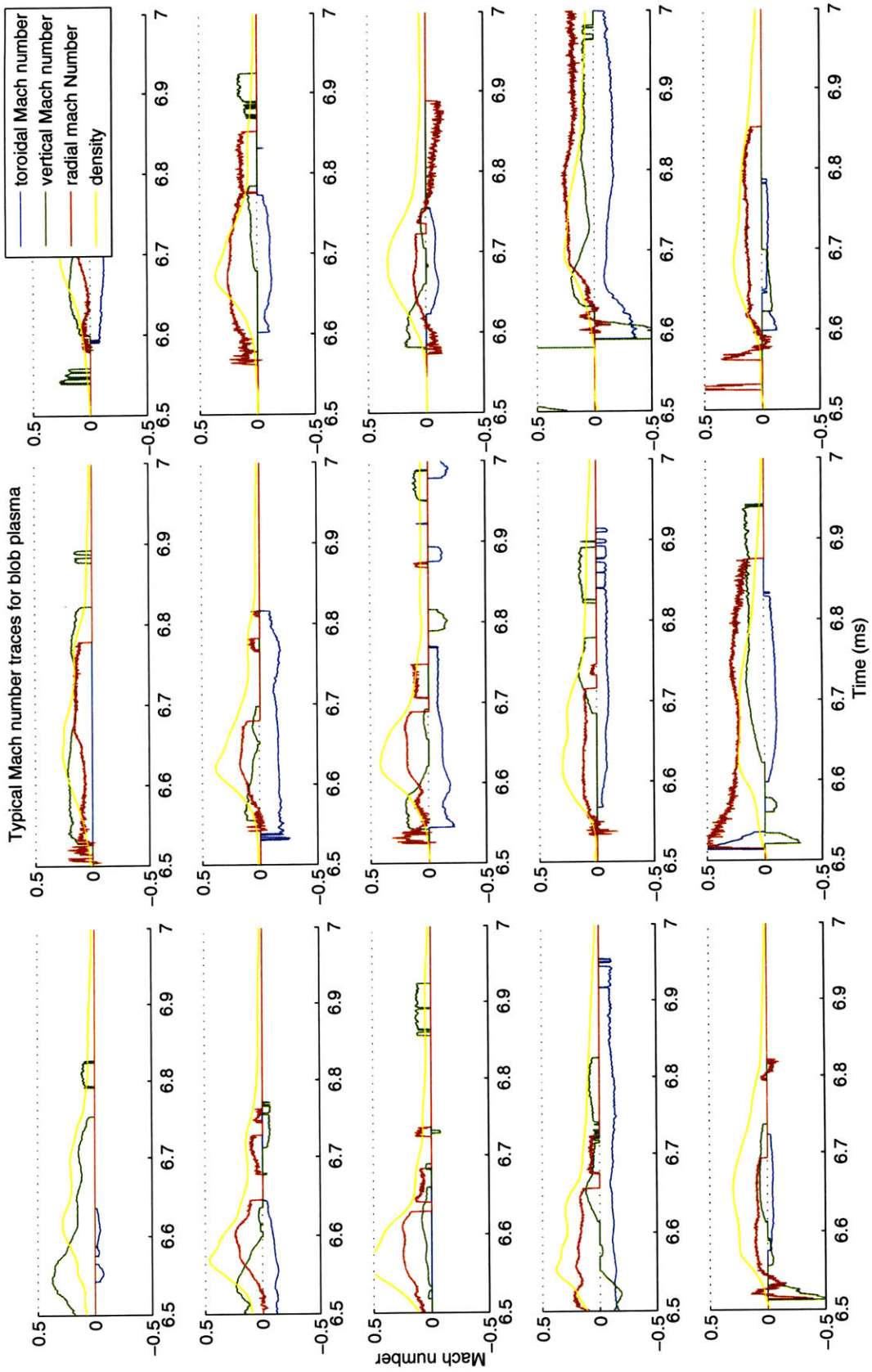

Figure 4-4: Typical Mach number traces from a blob passing across the Mach probe array. The density (in arbitrary units) is also plotted for reference.

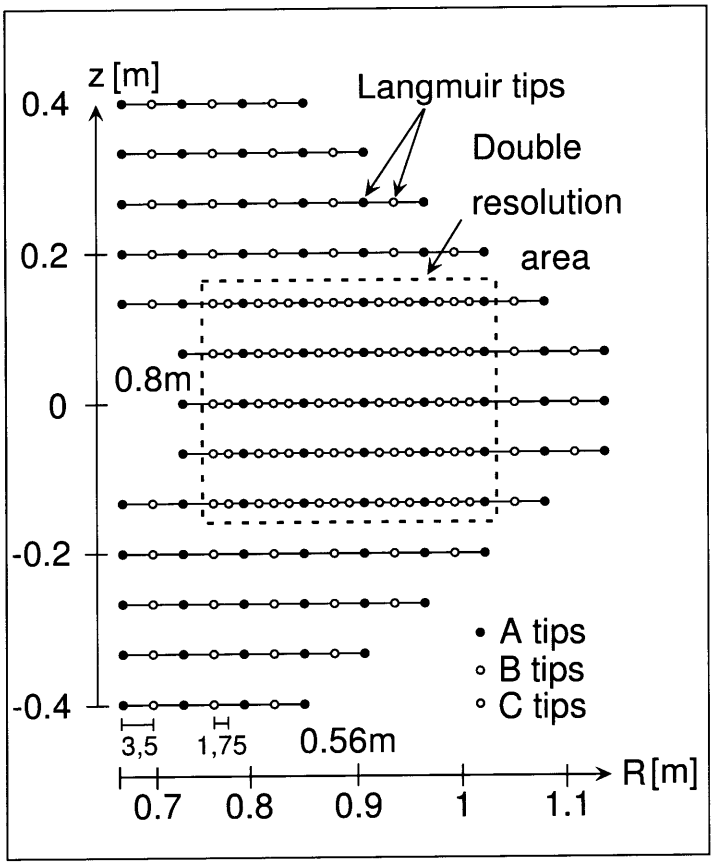

Figure 4-5: A diagram of the 200-tip Langmuir probe array. The A, B, and C tips are distinguished only by the applied probe bias in some modes of array operation.

data for low signal to noise (a discussion of this and other processing steps can be found in Chapter 4.1).

4.2.2 Calibration of Mach probe with Langmuir data

An array of 200 Langmuir probes installed on a cross section of the vessel at another toroidal angle provide a dataset that can be used to calibrate the Mach probe array. Like the Mach probes, the Langmuir probes are operated in the ion saturation region of their I-V curves; that is, they are biased to a very negative voltage compared to the plasma potential such that only the ion current is collected. The Langmuir array is diagrammed in Figure 4-5 The Langmuir probe array provides a measurement of the blob speed through the chamber by tracking the center of mass over time. I assume

here that the center of mass speed v_{CM} is a reasonable approximation of the flow velocity near the center of the blob. Therefore, by amassing corresponding datasets of v_{CM} and M_{peak} for the same plasma blobs, it will be possible to scale the M_{peak} data by a factor (presumably an approximation of the ion sound speed c_s) to match the Langmuir center of mass speed data. That comparison is shown in Figure 4-6 for three different neutral fill pressures (the pressure of the gas through which the plasma blob moves). From Figure 4-6, we can see that the Mach probe measurements, once fit to the Langmuir speed data, are a remarkably consistent measure of the blob velocity. There are a few notable features of the Mach probe data which should be addressed. First, in the medium pressure regime, the measured Mach velocity seems to be positively correlated with shot number. A likely explanation for this effect is that the plasma is more reproducible after the first several shots; it is possible that the blob speed does in fact increase over the first few shots due to some initial effect as the chamber equilibrates with the plasma conditions induced during the blob shots. The possibility of probe face contamination was considered, but it is unlikely that contamination could produce that effect; probe face contamination would decrease the collected current to both faces of each Mach probe by approximately the same factor $\alpha < 1$, and the measured Mach number should therefore be insensitive to contamination:

$$M_{contaminated} = \frac{\alpha j_{up} - \alpha j_{down}}{\alpha j_{up} + \alpha j_{down}} = \frac{j_{up} - j_{down}}{j_{up} + j_{down}} \tag{4.5}$$

$$= M_{clean} \tag{4.6}$$

Additionally, the low-pressure regime especially shows a systematic offset between the Mach data and the Langmuir data. Therefore, the Mach speeds were recalibrated, this time with a different factor for each pressure regime. The changes in the scaling factors likely represent, at least in part, changes in the sound speed due to differing T_e between blobs created at different pressure levels. The results of the three-part fit are shown in Figure 4-7. Once the scaling has been done individually for each neutral-pressure regime, the Mach numbers match more closely to the measured center of mass

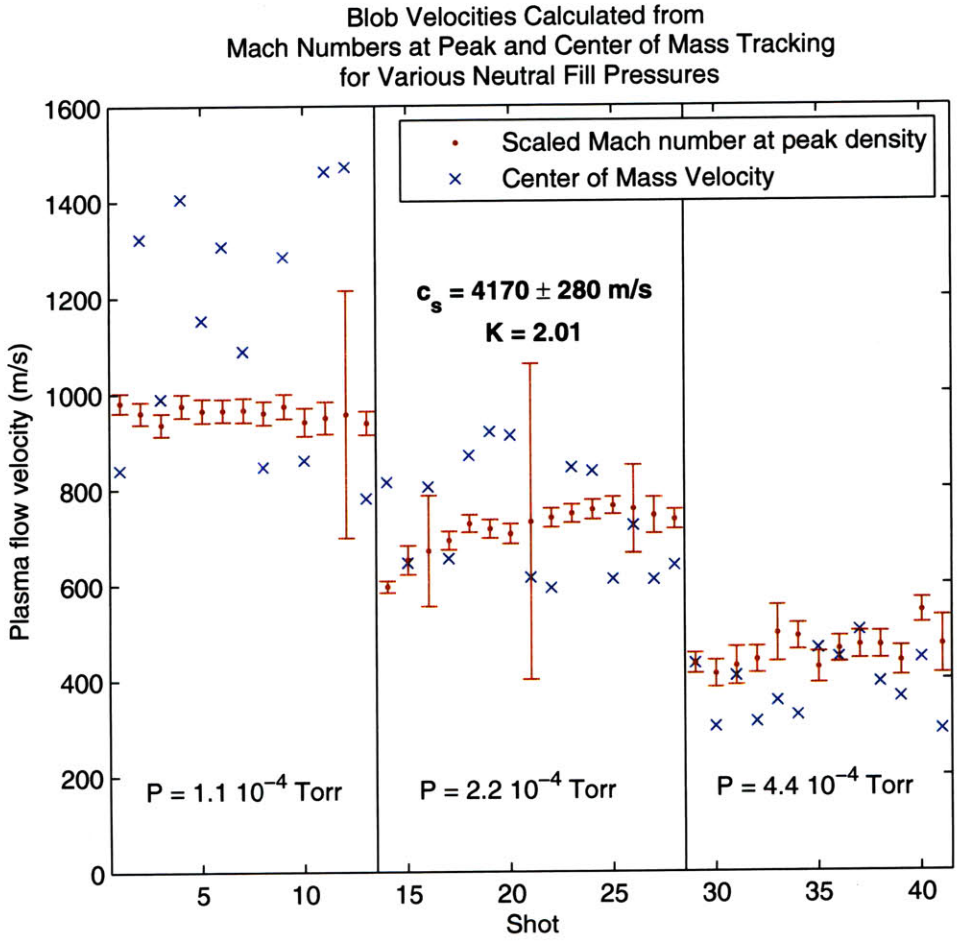

Figure 4-6: A comparison of Langmuir center of mass speeds and Mach numbers scaled by fitting the Mach numbers to the Langmuir data. Three different neutral pressure regimes are used, but all Mach numbers are scaled by the same factor. The factor is interpreted as the ion sound speed c_s. The plasma shots are approximately consecutive, separated by a few minutes.

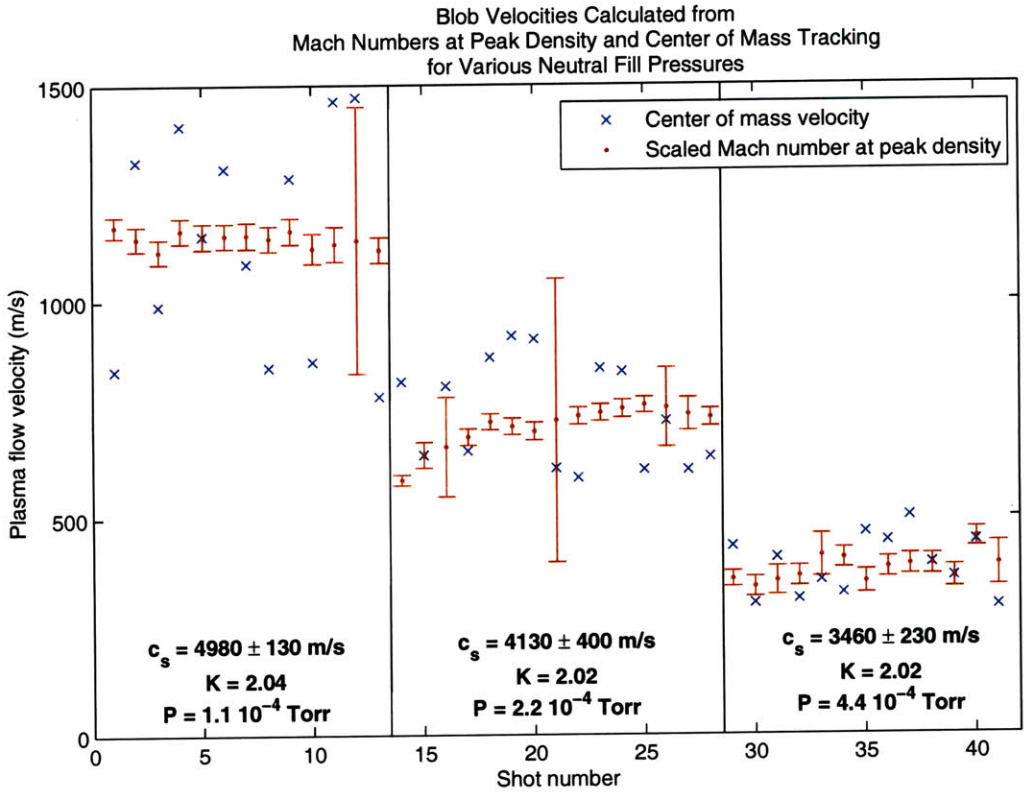

Figure 4-7: A comparison of Langmuir center of mass speeds and Mach numbers scaled by fitting the Mach numbers to the Langmuir data. Three different neutral pressure regimes are used, and a different scaling is used for the Mach numbers at each neutral pressure; each factor is interpreted as the ion speed c_s for each regime. Additionally, the calibration constant K from Equation 3.10 is found from the fit.

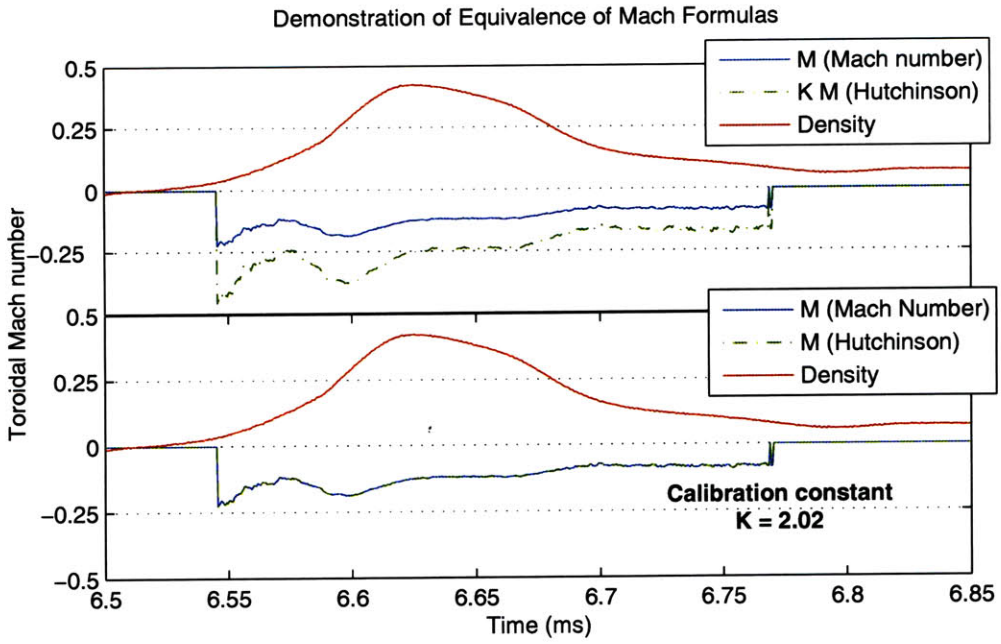

Figure 4-8: A representative ion flow trace is used to demonstrate that Equation 3.10 and Equation 3.13 are equivalent for $K = 2.02$. Note that in the lower axes, the dotted green trace is still present; it follows the blue trace very closely.

speed, and the systematic offset is eliminated. One very interesting finding from this analysis is the extremely good matching between the Mach numbers generated by the model given by Equation 3.10 and Equation 3.13; there is never more than a 0.5% disagreement in Mach number between the two. It is very interesting to note that the calculated calibration constant of $K \approx 2$ (as seen in Figure 4-7) varies very little over the three pressure regimes. This indicates that the simple model in Equation 3.13, which is equivalent for $K = 2$, is experimentally verified as a very reliable model, at least for this probe geometry and range of plasma conditions. The two Mach number sets were so close that it was impossible to display both in Figure 4-7. Figure 4-8 demonstrates the excellent agreement of the two models for $K = 2.02$.

4.2.3 Scaling of blob speed with neutral density

A recent study of plasma blobs in the VTF [4] has very accurately characterized the relationship between radial blob speed and the density of neutral gas surrounding the

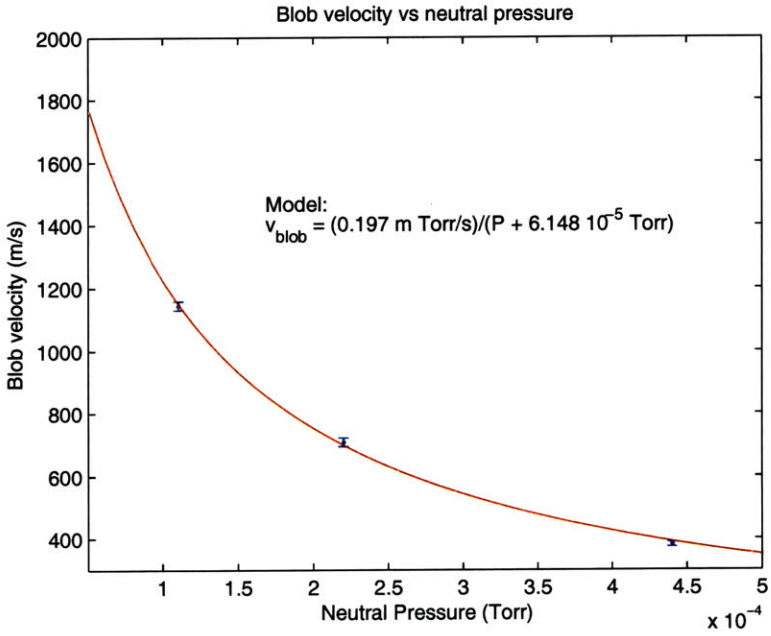

Figure 4-9: The inverse proportionality between neutral pressure and blob speed demonstrated theoretically and experimentally in [4] with the Langmuir array is verified using the Mach probe array data.

blobs. The same Langmuir array as employed in this thesis was used to precisely determine the structure and dynamics of the blobs. An illustration of the structure and propagation of the blobs taken from the study is show in Figure 2-4. Through analysis of the blobs at many different neutral pressures, it was experimentally established that the blob speed is inversely proportional to the neutral pressure. It was found that this relationship was theoretically supported by the equations of magnetohydrodynamics. The blobs are driven outwards by a ∇B drift, which corresponds to the centrifugal force on electrons as they are forced by the magnetic field to curve around the vessel toroidally [4]. However, the blobs also experience drag from the surrounding un-ionized argon gas. Using an average of the blob velocities calculated by the Mach probes for each pressure regime (see Figure 4-7), we have three points in the pressure-velocity space with which we can test this relationship. Figure 4-9 shows that the resulting fit is very good, and while it should be acknowledged that using three data points to verify a model with two degrees of freedom is not very impressive, the three available datapoints generated by the Mach probe array do agree with the previous study.

4.2.4 Toroidal flow

The blobs have proved themselves excellent plasma structures for the testing of the Mach probe array functionality. However, the array output indicated a curious property regarding the blobs; the Mach probes appear to be detecting a significant clockwise toroidal flow in the blobs, consistent in direction and approximately consistent in magnitude from shot to shot. That is, the blobs appear to be rotating, with a Mach number between 0.1 and 0.2. Figure 4-10 illustrates this toroidal flow with the Mach number data from a representative shot. There has been no satisfactory explanation for this rotation as of yet. The microwave heating source in the VTF is located in a port approximately 90^o counter-clockwise of the Mach array location, so unequal plasma creation due to an asymmetric heating source was considered as a source of the rotation. However, it is known from previous data that microwave reflections from the vessel walls in fact lead to axisymmetric plasma breakdown, so

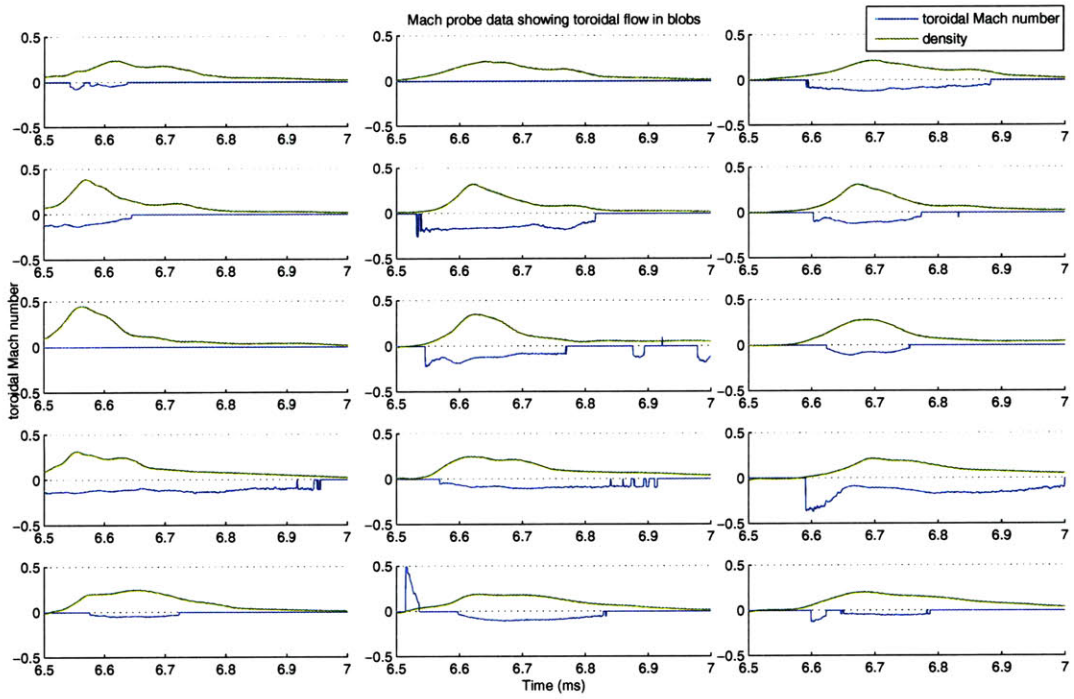

Figure 4-10: An unexplained clockwise toroidal flow of Mach number in the range 0.1 - 0.2 is consistently observed in plasma blobs. Note that there are two broken toroidal Mach probes in the upper left region of the array.

it is unlikely that the location of the microwave source is the cause. To eliminate the array construction or probe face contamination as a possible source of a spurious toroidal flow, the array was rotated 180^o about a vertical axis, such that the directions of the toroidal (as well as radial) probe faces had been flipped; the toroidal flow was again observed (in the same direction), strongly indicating that the blob plasma is in fact rotating clockwise.

Chapter 5

Conclusions

A Mach probe array was constructed and installed in the VTF plasma vessel. The method and materials of construction of the array were shown to be viable, although two probe faces out of the ninety in the array were found to have broken connections that could not be repaired; a stronger signal wire than the 0.004" diameter wire may be advisable for future array construction. Using plasma blobs created in the VTF, the operation of the array was verified. A 200-probe Langmuir probe array records poloidal density profiles of the blobs was used to create an independent reference dataset of blob speeds using center of mass. By comparison to this reference dataset from the Langmuir probe array, the Mach probe array could be calibrated, and in the process, the validity of several theories of Mach probe operation were evaluated.

It was found that the model proposed by Hutchinson and others in Equation 3.10 is valid for the blob plasma conditions, and that it was equivalent to a simpler model (Equation 3.13) for small Mach numbers such as those encountered in the blobs. Various analytical techniques for quantifying, reducing, or filtering out noise were developed, and a technique of correcting for the effects of plasma density gradients on the Mach probe data was advanced. Additionally, an apparent overall toroidal flow of the VTF blobs with Mach number of 0.1 - 0.2 was discovered from the Mach probe data. Finally, the inverse proportionality between blob speed and neutral pressure demonstrated in [4] was observed in the Mach probe data. The Mach probe, while presenting experimental and theoretical challenges, promises to be a valuable tool in

the study of complex plasma phenomena such as magnetic reconnection.

Appendix A

Tables

Table A.1: Mach number and ion speed data; this is Figure 4-7 in tabular form.

Shot #	Neutral pressure (10^{-4} Torr)	c_s (m/s)	Blob Mach number from Mach probes	Blob speed from Mach probes (m/s)	Blob speed from Langmuir probes (m/s)
1	1.1	4980	0.235	1172 ± 24	840
2	1.1	4980	0.230	1147 ± 28	1323
3	1.1	4980	0.224	1118 ± 28	989
4	1.1	4980	0.234	1165 ± 29	1406
5	1.1	4980	0.231	1152 ± 29	1152
6	1.1	4980	0.232	1153 ± 29	1307
7	1.1	4980	0.232	1154 ± 30	1088
8	1.1	4980	0.230	1146 ± 29	847
9	1.1	4980	0.234	1163 ± 30	1285
10	1.1	4980	0.226	1124 ± 35	861
11	1.1	4980	0.228	1134 ± 40	1463
12	1.1	4980	0.229	1142 ± 308	1472
13	1.1	4980	0.225	1120 ± 29	780
14	2.2	4130	0.143	591 ± 12	814
15	2.2	4130	0.156	646 ± 30	646
16	2.2	4130	0.161	664 ± 115	805
17	2.2	4130	0.166	686 ± 19	655
18	2.2	4130	0.174	720 ± 18	870
19	2.2	4130	0.172	710 ± 19	920
20	2.2	4130	0.169	699 ± 20	912
21	2.2	4130	0.175	724 ± 326	615
22	2.2	4130	0.177	732 ± 19	593
23	2.2	4130	0.179	741 ± 19	844
24	2.2	4130	0.181	748 ± 20	837
25	2.2	4130	0.183	757 ± 18	612
26	2.2	4130	0.182	750 ± 91	724
27	2.2	4130	0.178	737 ± 37	611
28	2.2	4130	0.176	728 ± 20	641
29	4.4	3460	0.104	360 ± 18	434
30	4.4	3460	0.099	342 ± 23	303
31	4.4	3460	0.103	356 ± 33	408
32	4.4	3460	0.106	366 ± 23	313
33	4.4	3460	0.119	412 ± 49	356
34	4.4	3460	0.118	407 ± 23	326
35	4.4	3460	0.102	353 ± 27	465
36	4.4	3460	0.111	384 ± 23	446
37	4.4	3460	0.113	391 ± 24	502
38	4.4	3460	0.113	391 ± 24	395
39	4.4	3460	0.105	363 ± 25	363
40	4.4	3460	0.130	451 ± 22	445
41	4.4	3460	0.113	392 ± 50	296

Bibliography

[1] T. J. M. Boyd and J. J. Sanderson. *The Physics of Plasmas.* Cambridge University Press, New York, 2003.

[2] Akira Ando et. al. Evaluation of mach probe characteristics and measurement of high-mach-number plasma flow. *Thin Solid Films*, pages 506–507, 2006.

[3] B. J. Peterson et. al. Measurement of ion flows using an 'unmagnetized' mach probe in the interchangeable module stellarator. *Rev. Sci. Instrum.*, 65(8):506–507, August 1994.

[4] Noam Katz et. al. Experiments on the propagation of plasma filaments. *Submitted to Phys. Rev. Letter*, 2008.

[5] T. Shikama et. al. Investigation of mach probe geometry effects in weakly magnetized plasmas. *Journal of Nuclear Materials*, pages 1077–1081, 2005.

[6] Martin Hudis and L. M. Lidsky. Directional langmuir probe. *Journal of Applied Physics*, 41(12):5011–5017, November 1970.

[7] Ian H. Hutchinson. The invalidity of a mach probe model. *Physics of Plasmas*, 9(5):1832–1833, May 2002.

[8] Ian H. Hutchinson. Ion collection by a sphere in a flowing plasma. *Plasma Phys. Control. Fusion*, 44:1953–1977, 2002.

[9] Ian H. Hutchinson. *Principles of Plasma Diagnostics.* Cambridge University Press, New York, second edition, 2002.